

# Spin-Dependent Recombination between Phosphorus Donors in Silicon and Si/SiO<sub>2</sub> Interface States Investigated with Pulsed Electrically Detected Electron Double Resonance

Felix Hoehne,<sup>\*</sup> Hans Huebl,<sup>†</sup> Bastian Galler, Martin Stutzmann, and Martin S. Brandt  
*Walter Schottky Institut, Technische Universität München, Am Coulombwall 3, 85748 Garching, Germany*  
 (Dated: April 2, 2024)

We investigate the spin species relevant for the spin-dependent recombination used for the electrical readout of coherent spin manipulation in phosphorus-doped silicon. Via a multi-frequency pump-probe experiment in pulsed electrically detected magnetic resonance, we demonstrate that the dominant spin-dependent recombination transition occurs between phosphorus donors and Si/SiO<sub>2</sub> interface states. Combining pulses at different microwave frequencies allows us to selectively address the two spin subsystems participating in the recombination process and to coherently manipulate and detect the relative spin orientation of the two recombination partners.

PACS numbers: 71.55.Cn, 76.30.-v, 03.67.Lx, 73.50.Gr

Electron spin resonance (ESR) is a well known tool to manipulate electron spins in semiconductors. Due to the limited detection sensitivity of ESR [1], typically electrical [2, 3] and optical detection schemes of spin resonance [4, 5] are favored to detect small numbers of spins. In both approaches, the spin state is transferred to a charge or photon state, respectively, and in electrical [6] as well as in optical detection [7], the coherent manipulation of spin states can be monitored. In spin-dependent photoconductivity, the spin-to-charge transfer is typically achieved via a spin-dependent process governed by the Pauli principle involving two paramagnetic states. While we can in principle distinguish between weakly and strongly coupled spin pairs via the Rabi frequencies [8], the identification of correlated states has only been achieved indirectly in electrically detected magnetic resonance (EDMR) until now [9, 10]. In this paper, we demonstrate that pulsed EDMR can be used to directly identify the partners participating in a recombination process. This is achieved by individually addressing the different partners during the EDMR pulse sequence via irradiation with microwaves at different frequencies.

We have performed this proof-of-principle experiment on an example of current interest for EDMR, the readout of phosphorus donor spin states in Si [11]. Prominent signatures of a continuous wave (cw) experiment on heterostructures of phosphorus-doped Si and SiO<sub>2</sub> used for such a read-out can be attributed to <sup>31</sup>P donor spins and dangling bond states P<sub>b0</sub> at the Si/SiO<sub>2</sub> interface [12]. Sometimes, a weak feature at  $g = 1.999(1)$ , compatible with the spin resonance of conduction band electrons or exchange coupled <sup>31</sup>P donors, is observed as well [13, 14]. A particular model for the spin-dependent process monitored in these experiments is the transition from the <sup>31</sup>P

donor to the P<sub>b0</sub> state as sketched in Fig. 1 a) [11]. An alternative process is depicted in Fig. 1 b), showing the parallel spin-dependent transition from conduction band electrons, denoted e, to the <sup>31</sup>P donors and the P<sub>b0</sub> centers, which would result in a similar cw EDMR signature of Shockley-Read-Hall recombination [15]. However, other mechanisms that could give rise to the observed cw resonances can also be envisaged such as scattering of conduction electrons at neutral <sup>31</sup>P donors [16], capture and emission of conduction band electrons by neutral <sup>31</sup>P donors [17–19], donor-acceptor pair recombination [20] and tunneling between P<sub>b0</sub> states [18]. Using cw EDMR experiments only, an identification of the process is complicated and if at all can only be achieved e.g. by studying the dependence of the EDMR signal on magnetic field, temperature or dynamical parameters such as the phase shift observed in lock-in detection [9]. Here, we employ multi-frequency pulsed EDMR, similar to electron double resonance (ELDOR) techniques in conventional ESR, to perform pump-probe experiments identifying the dominant recombination partners.

Before describing the experimental results we will discuss the measurement scheme used in the experiments. As a result of the spin-dependent recombination processes sketched in Fig. 1, doubly occupied diamagnetic states are formed, which are either <sup>31</sup>P<sup>−</sup> or P<sub>b0</sub><sup>−</sup>. In both cases, the Pauli principle demands that these states are in a spin singlet. Therefore, initial pairs of recombination partners (be it <sup>31</sup>P-P<sub>b0</sub> or e-<sup>31</sup>P and e-P<sub>b0</sub> pairs) that are in an antiparallel spin state will recombine faster than parallel spin pairs, leading to an occupation of recombination partners with parallel spins higher than in equilibrium. In a pulsed single frequency magnetic resonance excitation scheme, one of the spin species is rotated selectively while the other remains unaltered if the two spins are weakly coupled. Therefore, parallel spin states are transformed to antiparallel states depending on the pulse length of the excitation pulse. As shown in the lower part of Fig. 1 d) for microwave pulses resonant with the P<sub>b0</sub> spins, the corresponding recombination rate will oscillate

<sup>\*</sup>corresponding author, email: hoehne@wsi.tum.de

<sup>†</sup>present address: Walther-Meissner-Institut, Bayerische Akademie der Wissenschaften, Walther-Meissner-Strasse 8, 85748 Garching, Germany

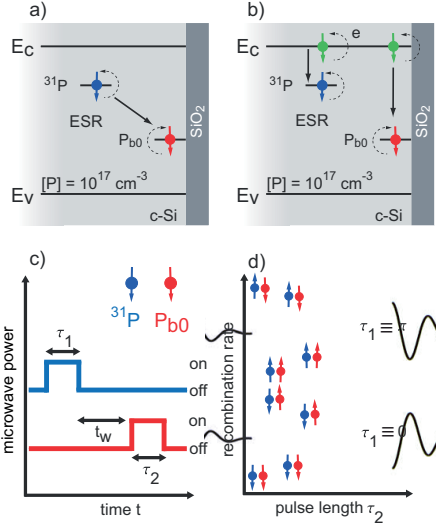


FIG. 1: (color online) a) Spin-dependent recombination step from the  $^{31}\text{P}$  donor to the  $\text{P}_{\text{b}0}$  center. In contrast, the recombination in b) involves conduction band electrons which spin-dependently recombine with  $^{31}\text{P}$  and  $\text{P}_{\text{b}0}$  not involving a direct transition between  $^{31}\text{P}$  and  $\text{P}_{\text{b}0}$ . c) Pulse scheme used in the multi-frequency pump-probe experiment. For the direct recombination involving  $^{31}\text{P}$  and  $\text{P}_{\text{b}0}$ , panel d) depicts the expected Rabi oscillations in the recombination rate induced by a probe pulse with length  $\tau_2$  on the  $\text{P}_{\text{b}0}$  spin system for two different starting conditions when no pump pulse and when a  $\pi$ -pump pulse has been applied to the  $^{31}\text{P}$  spin system.

as a function of the microwave pulse length  $\tau_2$  leading to Rabi oscillations. In particular at  $\tau_2 = 0$ , the recombination rate will be low due to the dominant parallel configuration. However, if a preceding microwave pulse selectively rotates the partner in the spin pair, the initial parallel/antiparallel configuration is changed, which is then reflected by a change of amplitude or even an inversion of the corresponding Rabi oscillations. As an example, for the case of a direct  $^{31}\text{P}$ - $\text{P}_{\text{b}0}$  recombination process the upper part of Fig. 1 d) shows the expected Rabi oscillations measured on the  $\text{P}_{\text{b}0}$  spins after inverting the  $^{31}\text{P}$  spins with a  $\pi$  pulse, which are inverted when compared to the Rabi oscillations when no initial pump pulse was applied to the  $^{31}\text{P}$  system. In contrast, if the recombination path is as indicated in Fig. 1 b), where the recombination is directly from the conduction band to either the  $^{31}\text{P}$  or  $\text{P}_{\text{b}0}$ , a preceding pulse on the spin species not involved in the spin-dependent recombination step (e.g. a pulse on the  $^{31}\text{P}$  when measuring the Rabi oscillations on the  $\text{P}_{\text{b}0}$ ) should not change the initial parallel/antiparallel ratio of the spin pair giving rise to the spin selection (the e- $\text{P}_{\text{b}0}$  pair in this example). Therefore, the Rabi oscillations should remain unchanged in this case.

The sample investigated is a 15 nm thick silicon layer with (001) surface doped with phosphorus at  $[\text{P}] = 10^{17} \text{ cm}^{-3}$  grown on top of a 500 nm thick nominally intrinsic buffer deposited by chemical vapor de-

position on a Si:B wafer (30  $\Omega\text{cm}$ ) [21]. The EDMR measurements were performed for a magnetic field of  $B_0 || [110]$  in a Bruker ESR dielectric microwave resonator with a quality factor of  $Q \approx 100$  at 6 K under illumination with the white light of a tungsten lamp. In the cw EDMR spectrum shown in Fig. 2 a) we observe two  $^{31}\text{P}$  donor lines with  $g = 1.9985$  and a hyperfine (hf) splitting of  $\approx 4.2 \text{ mT}$  [14] and two  $\text{P}_{\text{b}0}$  resonances at  $g = 2.005(1)$  and  $2.009(1)$  [12]. The pulsed experiments were performed at a constant  $B_0 \approx 349.1 \text{ mT}$  using three different microwave frequencies to excite magnetic resonance, one for the  $g = 2.005$   $\text{P}_{\text{b}0}$  resonance ( $f_{\text{P}_{\text{b}0}} = 9.7938 \text{ GHz}$ ) spectrally better resolved from the low-field  $^{31}\text{P}$  resonance and two for the two  $^{31}\text{P}$  hyperfine-split lines ( $f_{\text{P}_h} = 9.70508 \text{ GHz}$ ,  $f_{\text{P}_l} = 9.8202 \text{ GHz}$ ). The corresponding spectral positions in the cw EDMR spectrum are marked in Fig. 2 a). The two microwave frequencies for the hyperfine-split  $^{31}\text{P}$  resonances are adjusted in intensity to obtain matching Rabi frequencies corresponding to a  $\pi$  pulse time of  $\approx 37 \text{ ns}$ , longer than the shortest possible pulse length of 20 ns in our setup. For electrical access, interdigit Cr/Au contacts with 20  $\mu\text{m}$  contact distance define the active area of the device with  $2 \times 2.25 \text{ mm}^2$ , corresponding to approximately  $10^{10}$  P spins. During the experiment the metal-semiconductor-metal structure is biased in the ohmic region with 22 mV, resulting in a current of  $\approx 50 \mu\text{A}$ . The amplified current transient induced by the microwave pulses is high-pass filtered ( $f_{3\text{dB}} = 30 \text{ kHz}$ ) and recorded with a digital storage oscilloscope. To obtain a sufficient signal-to-noise ratio, the experiment is repeated with a repetition time of 250  $\mu\text{s}$  which is large compared to typical relaxation times [10, 22]. The recorded current transients are box-car integrated from 2 – 11  $\mu\text{s}$ , giving an integrated charge  $\Delta Q$  which is directly proportional to the recombination rate at the end of the microwave pulse sequence [11, 23].

We now apply the pump-probe sequence sketched in Fig. 1 c). The first pulse with length  $\tau_1$  addresses both hyperfine-split  $^{31}\text{P}$  ensembles. After  $t_w = 30 \text{ ns}$ , the second pulse with length  $\tau_2$  is applied at the  $\text{P}_{\text{b}0}$  resonance frequency. In Fig. 2 the integrated current transient is plotted as a function of  $\tau_2$  for different pulse lengths  $\tau_1$  of the preparation pulse. For  $\tau_1 = 0 \text{ ns}$  we observe Rabi oscillations on the  $\text{P}_{\text{b}0}$  center as expected from previous experiments [11]. The decay time constant of 250 ns can be attributed mainly to the inhomogeneity of the microwave  $B_1$  field in our resonator. When we change  $\tau_1$  to 37 ns, which corresponds to a  $\pi$  pulse on the P donor spins, we see an inversion of the Rabi oscillations on the  $\text{P}_{\text{b}0}$ . A further increase of  $\tau_1$  to 76 ns ( $\approx 2\pi$ ) again inverts the Rabi oscillations, resembling the situation for  $\tau_1 = 0 \text{ ns}$ . This oscillatory behavior continues for  $\tau_1$  times up to 146 ns ( $\approx 4\pi$ ).

Figure 3 a) shows the amplitude of the Rabi oscillations  $\delta Q$  as defined in Fig. 2 b) on the  $\text{P}_{\text{b}0}$  center as a function of the pulse length  $\tau_1$  (black solid squares). To extract the Rabi amplitude  $\delta Q$  from the data in Fig. 2,

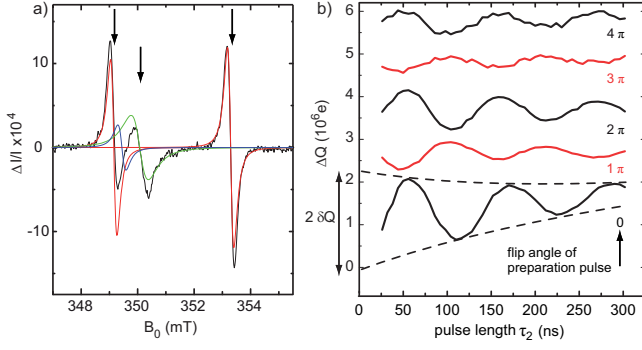


FIG. 2: (color online) a) Swept-field cw EDMR spectrum of the relative current change  $\Delta I/I$  (black line) at 6 K showing the two  $^{31}\text{P}$  hyperfine lines (red) and the two  $\text{P}_{\text{b}0}$  lines (blue and green). The colored lines are fits using a derivative Lorentzian line shape. In b), Rabi oscillations of the  $\text{P}_{\text{b}0}$  spins for several flipping angles of the first pulse on both  $^{31}\text{P}$  resonances in multiples of  $\pi$  are depicted. The Rabi oscillations for  $\tau_1 \equiv \pi$  and  $\tau_1 \equiv 3\pi$  are inverted (solid red lines) as expected for a spin-dependent recombination involving these two spin species.

each oscillation is fitted by an exponentially damped cosine plus a linear background. The Rabi amplitudes  $\delta Q$  oscillate with a period of  $75.7 \pm 1.3$  ns and decrease exponentially with increasing pulse length  $\tau_1$ . This oscillation period is in good agreement with the single frequency Rabi oscillations  $\Delta Q$  excited on the two hyperfine-split  $^{31}\text{P}$  resonances without a subsequent pulse on the  $\text{P}_{\text{b}0}$  spins ( $\tau_2 = 0$ ) shown in Fig. 3 b) with an oscillation period of  $73.7 \pm 0.5$  ns.

The clear inversion of the Rabi oscillations measured on  $\text{P}_{\text{b}0}$  indicates that the formation and recombination of pairs involving  $^{31}\text{P}$  and  $\text{P}_{\text{b}0}$  (Fig. 1 a)) is the spin-dependent recombination process observed in EDMR under the magnetic field and temperature conditions used here, in contrast to Ref. [18] which studies EDMR at 8 T. The quantitative analysis performed below allows us to conclude that within an error margin of  $\approx 10\%$  the EDMR signal amplitude observed is completely caused by this process.

The inverted Rabi oscillations for  $\tau_1 \equiv \pi$  and  $\tau_1 \equiv 3\pi$  in Fig. 2 have a smaller amplitude compared to those for  $\tau_1 \equiv 2\pi$  and  $\tau_1 \equiv 4\pi$  in contrast to the expected monotonous decay with longer pulse length  $\tau_1$ . This can also be seen in Fig. 3 a) as the constant contribution to the linear offset (dotted black line). There are two effects causing this incomplete inversion of the Rabi oscillations. First, the bandwidth of the microwave pulses is not sufficient to excite all spins of the inhomogeneously broadened  $^{31}\text{P}$  lines in our experimental setup. Therefore, after applying a  $\pi$  pulse most but not all of the spins of the  $^{31}\text{P}$  spin ensemble are turned by  $\pi$  as required for a full inversion of the Rabi oscillations on the  $\text{P}_{\text{b}0}$  spins. Since a small fraction of the  $^{31}\text{P}$  spin ensemble is not addressed by the pulse, the Rabi oscillations of a small part of the  $\text{P}_{\text{b}0}$  spin ensemble also does not change its sign. This

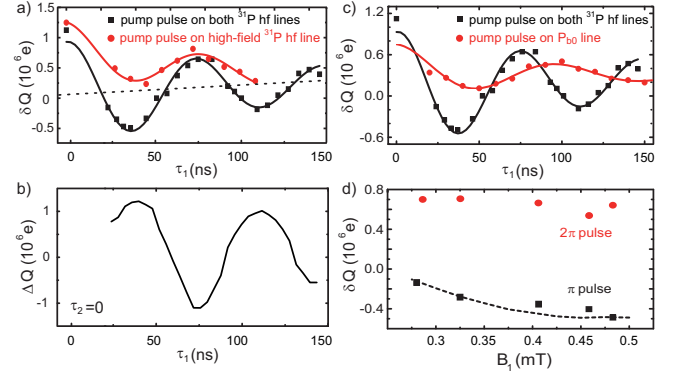


FIG. 3: (color online) Panel a) shows the amplitude  $\delta Q$  of the Rabi oscillations on the  $\text{P}_{\text{b}0}$  spins vs. the pulse length  $\tau_1$  of the pump pulse on both  $^{31}\text{P}$  resonances (black squares) and on the high-field  $^{31}\text{P}$  resonance only (red dots). The solid lines are fits with an exponentially damped cosine plus a linear background (black dotted line for excitation of both  $^{31}\text{P}$  resonances). b) Rabi oscillations excited on both  $^{31}\text{P}$  hyperfine lines without subsequent probe pulse. c) Comparison of  $\delta Q$  for pumping on both  $^{31}\text{P}$  lines (black) and on the  $\text{P}_{\text{b}0}$  resonance (red). d) Amplitude  $\delta Q$  of the Rabi oscillations on the  $\text{P}_{\text{b}0}$  spins as a function of the microwave  $B_1$  field amplitude of  $\pi$  and  $2\pi$  pump pulses on both  $^{31}\text{P}$  hyperfine lines. The dashed line is a numerical simulation taking power broadening effects into account.

can be demonstrated more clearly by limiting the pump pulses to irradiation with  $f_{\text{P}_h}$  only, thereby addressing half of the  $^{31}\text{P}$  system. As can be seen Fig. 3 a), the variation of  $\delta Q$  is now indeed about half of the variation when both  $^{31}\text{P}$  resonances are excited.

Second, the  $\text{P}_{\text{b}0}$  resonances are close to the low-field  $^{31}\text{P}$  line (see Fig. 2 a)), so that a pump pulse on both  $^{31}\text{P}$  hf lines partially also excites the  $\text{P}_{\text{b}0}$  spins. This also results in an incomplete inversion of the Rabi oscillations after a  $\pi$  pump pulse. To estimate this offset quantitatively, we describe the linewidths of the  $^{31}\text{P}$  resonances and the two  $\text{P}_{\text{b}0}$  resonances, which are in fact caused mostly by superhyperfine interactions with  $^{29}\text{Si}$  nuclei, by corresponding Gaussian distributions of  $g$ -factors with full width at half maximum of  $\Delta g_{\text{P}} = 0.001$ ,  $\Delta g_{\text{P}_{\text{b}0}} = 0.0016$  and  $\Delta g'_{\text{P}_{\text{b}0}} = 0.0008$ . From this, we estimate the fraction of  $^{31}\text{P}$  spins turned by a  $\pi$  pulse of 37 ns (corresponding to a microwave magnetic field  $B_1 = 0.48$  mT) to  $\approx 0.9$  and the fraction of  $\text{P}_{\text{b}0}$  spins to  $\approx 0.1$  which accounts for the constant offset in Fig. 3 a) quantitatively. This is corroborated by the pump experiments on the spectrally better resolved high-field  $^{31}\text{P}$  resonance only, where an amplitude of the oscillations of  $\delta Q$  of  $4.9 \times 10^5$  e is obtained from the fit in Fig. 3 a), while  $8.2 \times 10^5$  e is found when both  $^{31}\text{P}$  resonances are excited. Comparison of these two values allows to determine the fraction of  $\text{P}_{\text{b}0}$  spins turned by exciting the less resolved  $^{31}\text{P}$  resonance to  $\approx 0.2$  in reasonable agreement with the value estimated earlier. This discussion shows that higher magnetic fields  $B_0$  removing the

spectral overlap of resonances would be beneficial.

Furthermore, the model is supported by repeating the experiment at lower powers of the microwave pulses on the two  $^{31}\text{P}$  ensembles as shown in Fig. 3 d). The amplitude  $\delta Q$  after a  $\pi$  pump pulse decreases with decreasing  $B_1$  field whereas it remains almost constant for a  $2\pi$  pump pulse as expected. The lower  $B_1$  fields lower the fraction of  $^{31}\text{P}$  spins affected by the pulses which reduces the inversion. The dashed line is a numerical simulation taking these power broadening effects into account. The origin of the additional slight increase of the background in Fig. 3 a) can similarly at least qualitatively be explained taking into account that the spectral width of the microwave pulses decreases with increasing pulse length also when keeping the microwave power constant. Therefore, the fraction of  $^{31}\text{P}$  spins addressed by the pulses is reduced when  $\tau_1$  is increased resulting in an increasing background.

If the  $^{31}\text{P}$ - $\text{P}_{\text{b0}}$  spin pair recombination indeed takes place, an exchange of the  $^{31}\text{P}$  and  $\text{P}_{\text{b0}}$  pulses in the pulse sequence should result in the same pulsed EDMR signature. We performed this experiment by applying the pump pulse to the  $\text{P}_{\text{b0}}$  spin species and monitoring Rabi oscillations on the high-field  $^{31}\text{P}$  resonance. As shown in Fig. 3 c), the amplitude  $\delta Q$  of the Rabi oscillations on  $^{31}\text{P}$  oscillates with a period of  $\approx 100$  ns characteristic for the length of  $2\pi$  pulses on the  $\text{P}_{\text{b0}}$  system (c.f. Fig. 2 b)). However, also in this case no inversion of the Rabi oscillations after a  $\pi$  pulse was observed. The  $g$ -factor distribution of the two  $\text{P}_{\text{b0}}$  lines is wider compared to the  $^{31}\text{P}$  spins and therefore only a smaller fraction of  $\approx 0.5$  of all  $\text{P}_{\text{b0}}$  spins is addressed by the first microwave pulse preventing an inversion of the Rabi oscillations.

Two models to account for the relative current change  $\Delta I/I$  detected in cw EDMR experiments are usually discussed, the Lepine model [24] based on the polarisation of the spin species participating and the Kaplan-Solomon-Mott model [25] assuming weakly coupled pairs. While

the experiments reported here clearly demonstrate that the spin-dependent recombination step we monitor in the Si:P epilayers takes place between the  $^{31}\text{P}$  and the  $\text{P}_{\text{b0}}$  center, we cannot make conclusions on the coupling from these experiments. Most likely, exchange interaction caused by an overlap of the two wavefunctions leads to this coupling. However, also an indirect coupling e.g. by itinerant charge carriers such as electrons or holes cannot be excluded at this point. However, together with the recently demonstrated capability to refocus the spin system and observe recombination echoes electrically [10] the multi-frequency pulsed EDMR reported here will allow e.g. to measure the  $^{31}\text{P}$ - $\text{P}_{\text{b0}}$  spin coupling via the Double Electron Electron Resonance pulse scheme. A sample with a sufficiently narrow distribution of  $^{31}\text{P}$ - $\text{P}_{\text{b0}}$  coupling strengths thus determined might allow to demonstrate the elemental two qubit operation, the CNOT, between the electron spins of the phosphorus donor and the  $\text{P}_{\text{b0}}$  interface state.

To summarize, we have used pulsed electrically detected electron double resonance to investigate the spin-dependent recombination in phosphorus doped crystalline silicon. In the pump-probe experiment performed, we show that the rotation of the  $^{31}\text{P}$  spins by a pump pulse results in an oscillating amplitude of the Rabi oscillations detected on the  $\text{P}_{\text{b0}}$  center and vice versa. In particular, using a  $\pi$  pump pulse on both  $^{31}\text{P}$  resonances we observe an inversion of the Rabi oscillations on the  $\text{P}_{\text{b0}}$  line. This interplay of the two spin species clearly demonstrates that the spin-dependent recombination proceeds between the phosphorus donor and a  $\text{P}_{\text{b0}}$  center. The technique shown here is not limited to this specific spin system, but can be applied in general to identify the partners participating in spin-dependent transport processes.

The authors would like to thank A. R. Stegner for fruitful discussions. The work was financially supported by DFG (Grant No. SFB 631, C3).

- 
- [1] D. C. Maier, Bruker Rep. **144**, 13 (1997).
  - [2] F. H. L. Koppens, C. Buizert, K. J. Tielrooij, I. T. Vink, K. C. Nowack, T. Meunier, L. P. Kouwenhoven, and L. M. K. Vandersypen, Nature **442**, 776 (2006).
  - [3] D. R. McCamey, H. Huebl, M. S. Brandt, W. D. Hutchison, J. C. McCallum, R. G. Clark, and A. R. Hamilton, Appl. Phys. Lett. **89**, 182115 (2006).
  - [4] J. Koehler, J. A. J. M. Disselhorst, M. C. J. M. Donckers, E. J. J. Groenen, J. Schmidt, and W. E. Moerner, Nature **363**, 242 (1993).
  - [5] J. Wrachtrup, C. von Borczykowski, J. Bernard, M. Orrit, and R. Brown, Nature **363**, 244 (1993).
  - [6] C. Boehme and K. Lips, Phys. Rev. Lett. **91**, 246603 (2003).
  - [7] L. Childress, M. V. G. Dutt, J. M. Taylor, A. S. Zibrov, F. Jelezko, J. W. P. R. Hemmer, and M. D. Lukin, Science **314**, 281 (2006).
  - [8] T. W. Herring, S.-Y. Lee, D. R. McCamey, P. C. Taylor, K. Lips, J. Hu, F. Zhu, A. Madan, and C. Boehme, Phys. Rev. B **79**, 195205 (2009).
  - [9] H. Dersch, L. Schweitzer, and J. Stuke, Phys. Rev. B **28**, 4678 (1983).
  - [10] H. Huebl, F. Hoehne, B. Grolik, A. R. Stegner, M. Stutzmann, and M. S. Brandt, Phys. Rev. Lett. **100**, 177602 (2008).
  - [11] A. R. Stegner, C. Boehme, H. Huebl, M. Stutzmann, K. Lips, and M. S. Brandt, Nature Physics **2**, 835 (2006).
  - [12] A. Stesmans and V. V. Afanas'ev, J. Appl. Phys. **83**, 2449 (1998).
  - [13] C. F. Young, E. H. Poindexter, G. J. Gerardi, W. L. Warren, and D. J. Keeble, Phys. Rev. B **55**, 16245 (1997).
  - [14] G. Feher, R. C. Fletcher, and E. A. Gere, Phys. Rev. **100**, 1784 (1955).
  - [15] W. Shockley and W. T. Read, Phys. Rev. **87**, 835 (1952).
  - [16] R. N. Ghosh and R. H. Silsbee, Phys. Rev. B **46**, 12508 (1992).

- [17] D. D. Thornton and A. Honig, Phys. Rev. Lett. **30**, 909 (1973).
- [18] D. R. McCamey, G. W. Morley, H. A. Seipel, L. C. Brunel, J. van Tol, and C. Boehme, Phys. Rev. B **78**, 045303 (2008).
- [19] G. W. Morley, D. R. McCamey, H. A. Seipel, L.-C. Brunel, J. van Tol, and C. Boehme, Phys. Rev. Lett. **101**, 207602 (2008).
- [20] B. Stich, S. Greulich-Weber, and J.-M. Spaeth, J. Appl. Phys. **77**, 1546 (1995).
- [21] H. Huebl, A. R. Stegner, M. Stutzmann, M. S. Brandt, G. Vogg, F. Bensch, E. Rauls, and U. Gerstmann, Phys. Rev. Lett. **97**, 166402 (2006).
- [22] S.-Y. Paik, S.-Y. Lee, W. J. Baker, D. R. McCamey, and C. Boehme, arXiv:0905.0416v1 (2009).
- [23] C. Boehme and K. Lips, Phys. Rev. B **68**, 245105 (2003).
- [24] D. J. Lepine, Phys. Rev. B **6**, 436 (1972).
- [25] D. Kaplan, I. Solomon, and N. F. Mott, J. Phys. (Paris) **39**, L51 (1978).